PHILOSOPHICAL TRANSACTIONS OF THE ROYAL SOCIETY A MATHEMATICAL, PHYSICAL & ENGINEERING SCIENCES

Ionization Fronts in Interstellar Gas and the Expansion of HII Regions

F. A. Goldsworthy

Phil. Trans. R. Soc. Lond. A 1961 **253**, 277-300
doi: 10.1098/rsta.1961.0001

IONIZATION FRONTS IN INTERSTELLAR GAS AND THE EXPANSION OF HII REGIONS

By F. A. GOLDSWORTHY

Department of Mathematics, University of Manchester

(*Communicated by M. J. Lighthill, F.R.S.—Received* 11 *April* 1960)

CONTENTS

The gas dynamical effects of an expanding nearly fully ionized hydrogen region (HII region), which is associated with the formation of *O* and *B* stars, are investigated. The radiation from the hot star is absorbed by the surrounding interstellar gas (mainly neutral hydrogen) and leads to its ionization. Previous analyses have disregarded the internal motions set up in expanding HII regions. Similarity solutions of the equations of motion are presented for spherical and cylindrical problems, thus enabling the effects of groups of stars as well as individual stars to be discussed. For similarity to be applicable the initial density variations of the undisturbed neutral gas have to be like $1/r^{\frac{3}{2}}$ in the spherical case and like $1/r$ in the cylindrical case. This does not, however, limit their use in describing the general picture of events for any other given density distribution. Recombination of the ions and electrons and subsequent re-ionization by radiation within the HII region is allowed for; cooling processes such as that due to the excitation of O^+ ions are also taken into account. It is shown that the temperature of the ionized gas in the HII region is approximately uniform even though the region as a whole is expanding. Rates of expansion are calculated and it is also determined whether a shock propagates ahead of the ionized gas. In particular for rates of expansion less than about 20 km/s a shock wave occurs ahead, but for speeds greater than about 20 km/s, which would occur in the initial motion, the rate of expansion of the ionized gas is too great and an 'isothermal' shock occurs within the HII region. The boundary between the ionized and neutral gases can be regarded as a discontinuity and is termed an ionization front. The present paper is concerned with the propagation of such fronts and accompanying shocks; a companion paper by W. I. Axford investigates the structures of 'isothermal shock' and ionization fronts. The lack of uniqueness, which occurs in the present paper, is removed when the results are combined with Axford's work.

1. Introduction

The gas dynamical effects arising from the absorption of ionizing radiation from a hot star in surrounding interstellar gas have been considered by several authors. Strömgren (1939) discussed the static problem and found that interstellar gas can roughly be divided into regions of neutral atomic hydrogen (hereafter referred to as the HI regions) and regions of nearly complete ionized hydrogen (HII regions) near the radiating stars. Strömgren

investigated the extent of the H II region and the boundary between it and an H I region. The static H II region is referred to as the Strömgren sphere and it is shown that, for an initial number density of n_0 hydrogen atoms per cubic centimetre, the radius of the Strömgren sphere is proportional to $n_0^{-\frac{2}{3}}$. He found that the transition from high to low ionization occurs in a very narrow region, in which as the proportion of neutral atoms increases the absorption of the ionizing radiation becomes more intense. The thickness of this region is small compared with the radius of the Strömgren sphere and hence can be regarded as a discontinuity. In the treatment of expanding H II regions this is a convenient assumption to make as it leads to considerable simplification of the problem without losing many of its essentials. The discontinuity is termed an ionization front and exhibits similar properties to detonations and deflagrations. Some expressions connecting the flow variables on both sides of an ionization front have been obtained by Kahn (1954). He introduced the following nomenclature for the different kinds of ionization fronts. An *R*-type ionization front advances with supersonic speed relative to the neutral gas ahead, while a *D*-type ionization front advances with subsonic speed relative to the neutral gas. Thus an *R*-type ionization front corresponds to a detonation and a *D*-type ionization front to a deflagration. We shall use the same nomenclature but in addition we shall introduce the terms 'weak *D*-type and strong *R*-type' or 'strong *D*-type and weak *R*-type' according to whether the ionization front moves with subsonic or supersonic speed relative to the ionized gas behind the front, respectively. A full discussion of the structure and properties of *R*- and *D*-type ionization fronts is given by Axford in the following paper. Though we use Kahn's nomenclature, the equations which he derived will be modified in the later stages of this paper to allow for recombination of ions and electrons and cooling effects in the vicinity of the ionization front. This leads to important differences in the properties of ionization fronts from those listed by Kahn; hence the reason for the more detailed investigation by Axford.

The heating and cooling of interstellar gas in both the H I and H II regions have been discussed by Spitzer, Savedoff and others, and for details reference should be made to a general lecture on the behaviour of interstellar gas given by Spitzer (1953). They concluded that in the H II region the main processes involved are:

(i) the absorption of a stellar photon of high energy by a neutral atom, with the electron going off with high kinetic energy which is available for heating the gas;

(ii) the recombination of the resulting electrons and ions;

(iii) the excitation of the 0^+ excited level, 3·31 eV above the ground state.

The re-emission of radiation in the gas itself resulting from the recombination of electrons and ions will be neglected in this paper in order to simplify the problem. The last two processes will cool the gas. Spitzer and his co-workers found that for the heating and cooling processes to balance, the temperature in the H II region must be in the neighbourhood of 7000 to 10 000 °K. The heating and cooling processes in the H I regions are different from the above and are more complicated but a rough estimate of 100 °K for the equilibrium temperature appears to be acceptable.

In this paper we shall consider the motion of a cloud of interstellar gas which is suddenly exposed to a stream of ionizing radiation from a star or group of stars embedded in it. An H II region will result and this will expand and push the neutral atomic hydrogen gas ahead of it. It will be shown in this paper that if its rate of expansion is less than about

20 to 25 km/s (depending on the type of radiating star) then a shock wave will propagate ahead of the ionization front. Kahn & Schatzman (1955) considered a simplified model based on Strömgren's formula holding in the H II region and assuming the shock and the ionization fronts to be close together. By application of the Rankine–Hugoniot shock relations they were able to deduce the speeds of the shock and the ionization fronts. Savedoff & Greene, unpublished, have considered the spherical problem in a manner similar to Taylor's (1946) consideration of the expansion of a shock wave surrounding a uniformly expanding sphere. The expanding sphere in their case was the expanding H II region; Strömgren's formula was applied to discuss its motion. In their analysis they allowed for the cooling of the gas behind the shock. Like Kahn & Schatzman they found that the expanding region is surrounded by a dense H I region separated from the undisturbed H I region by a shock front. In both the above-mentioned papers no attempt was made to discuss the internal motion of the H II region or to examine the changing pattern of the flow in the course of the expansion, for instance, to consider whether a shock always propagates ahead of the ionization front. Although a complete analysis of the problem is difficult, the present paper endeavours to make good this deficiency and seeks a fuller analysis of the whole flow, including the internal motion of the H II region. Thus the heating and cooling processes in the H II region as given by Spitzer are included and allowance is made for absorption of radiation from the star by recombined electrons and ions. Of necessity a similarity of the flow pattern at all times is resorted to in order to simplify the method of solution of the partial differential equations involved. This is an idealization but it does not, however, prevent one from making a general discussion of the change in the flow pattern as the H II region expands into any given initial density distribution of the neutral gas. In this paper the rates of expansion of H II regions and accompanying shocks, if any, are examined. We first neglect the effects of recombination and re-ionization in the H II region—this leads to the result that the temperature is zero at the star which is obviously wrong. It serves to stress the importance of considering the re-ionization of the recombined atoms by absorption of radiation. This heats the gas and prevents the preceding result. Two basic simplifying approximations are therefore made:

(i) the temperature of the H II region is assumed to be approximately uniform, and

(ii) the gas in the H II region is assumed to be nearly fully ionized.

Both these approximations are critically examined by Axford (1961) in the next paper. By investigating the structure of ionization fronts he is also able to settle the questions relating to the uniqueness of the flow pattern.

2. Equations of motion in the H II region

All flow variables are assumed to depend only on the distance r from the centre of the star and time t. A parameter n is introduced, which takes the value 1 or 2 according to whether cylindrical or spherical symmetry is assumed. The equations are so written in the hope that they will be self explanatory.

(i) Outward flux of quanta

$$-\frac{\partial}{\partial r}(Jr^n) = \alpha[Jr^n]\left[\frac{\rho}{M}(1-x)\right], \tag{1}$$

where J is the number of photons crossing unit area per second, α is the absorption coefficient for ionizing radiation (at the Lyman limit), ρ is the density, M is the mass of a hydrogen atom and x is the fraction of ionized atoms. The value of the absorption coefficient at the Lyman limit is $6{\cdot}3\times10^{-18}\,\mathrm{cm}^{-2}$ (see Allen 1955). Re-emission of quanta in the gas itself resulting from the recombination of electrons and ions has necessarily been neglected in order to preserve radial symmetry. Strömgren (1939) made the same approximation and gave reasons to justify it.

At the star, $r = R_*$, the photon output, $J_* R_*^n$, is a known constant.

(ii) Ionization balance equation

$$\frac{\mathrm{D}}{\mathrm{D}t}\left(\frac{\rho x}{M}\right)+\frac{\rho x}{M}\frac{1}{r^n}\frac{\partial}{\partial r}(r^n u) = \alpha J\left[\frac{\rho}{M}(1-x)\right]-\beta\left[\frac{\rho x}{M}\right]^2, \tag{2}$$

where $\mathrm{D}/\mathrm{D}t = \partial/\partial t + u\partial/\partial r$, u is the radial velocity of the gas and β is the recombination coefficient ($= 3\times10^{-10}/T^{\frac{3}{4}}\,\mathrm{cm}^3/\mathrm{s}$; see Allen 1955). The first term on the right-hand side represents the production of ions by the absorption of radiation from the star; the second term represents the loss of ions on recombination with electrons.

(iii) Equation of state

$$p = (k/M)\,\rho(1+x)\,T, \tag{3}$$

where p is the pressure, k is Boltzman's constant and T is the temperature.

(iv) Equation of momentum

$$\frac{\mathrm{D}u}{\mathrm{D}t} = -\frac{1}{\rho}\frac{\partial p}{\partial r}-\frac{G\mathscr{M}}{r^n}, \tag{4}$$

where $\mathscr{M}$ is the mass of the star or, in the case when approximate cylindrical symmetry exists, twice the mass per unit length of the axis along which a group of stars are supposed to be distributed.

(v) Conservation of matter

$$\frac{\partial\rho}{\partial t}+\frac{1}{r^n}\frac{\partial}{\partial r}(r^n\rho u) = 0. \tag{5}$$

(vi) Equation of energy

$$\rho\left\{\frac{\mathrm{D}}{\mathrm{D}t}\left(\frac{3}{2}\frac{p}{\rho}\right)+p\frac{\mathrm{D}}{\mathrm{D}t}\left(\frac{1}{\rho}\right)\right\} = \alpha J\left[\frac{\rho}{\mathrm{M}}(1-x)\right]\left[\tfrac{1}{2}MQ_0^2\right]-\beta\left[\frac{\rho x}{M}\right]^2\left[\tfrac{3}{2}kT\right]-\left[\frac{\rho x}{M}\right]^2 L_{ei}(T), \tag{6}$$

where $\frac{1}{2}MQ_0^2$ is the amount of energy left over, on the average, in each ionization. The second and third terms on the right-hand side of equation (6) represent the loss of heat in the gas by the recombination of ions with electrons and by the excitation of O^+ ions, respectively. $L_{ei}(T)$ is the energy lost per electron per second in collision with oxygen ions and this has been computed by Spitzer (1954) and for $T > 4000\,^\circ\mathrm{K}$ it can be approximated by the form

$$L_{ei}(T) = 0{\cdot}97\times10^{-31}\,(T-4000)^2 \tag{7}$$

In Spitzer's computation the electron density was set equal to 1 per cubic centimetre and the density of oxygen ions to 10^{-3} per cubic centimetre. In our calculations the electron density is $(\rho x)/M$. Since the first ionization potential of an oxygen atom (13·56 eV) is nearly the same as that of hydrogen (13·54 eV), we can expect that the density of oxygen ions will be proportional to the density of protons, $(\rho x)/M$. Observations by Struve and his colleagues (see Struve 1950) substantiate this assumption; they found that O^+ ions are almost

always present in regions where hydrogen is ionized and show the same sharp boundaries. We will assume the same abundance ratio of oxygen to hydrogen as that assumed by Spitzer, so that his results need only to be multiplied by $[(\rho x)/M]^2$ to obtain the energy lost per second per unit volume, i.e. the third term on the right-hand side of equation (6).

In deriving the above equations we have neglected the fact that the absorption coefficient of the H atom varies with the frequency of the radiation absorbed; photons of low frequency are removed more easily than photons of high frequency. This means that the average energy of the photons remaining increases as their number decreases. This effect has been discussed by Kahn (1954) and Pottasch (1958) with reference to the bright rims on diffuse nebulae. An approximate relation between the number of photons incident on unit area per second and the average amount of thermal energy liberated at one ionization was worked out. For the purposes of the present discussion, however, we will neglect the effect and take $\frac{1}{2}MQ_0^2$ to be a constant equal to kT_* (see Kahn 1954).

3. Equations of motion in the H I region

If the neutral gas is disturbed before ionization takes place then we must consider the motion set up in a hot H I region surrounding the expanding ionized gas. The equations of motion in the H I region are therefore the equations of momentum and continuity as given in §2, and the energy equation (6) with the right-hand side zero if cooling is neglected.

Initially the neutral gas is in gravitational equilibrium so that

$$\frac{1}{\rho_0}\frac{\mathrm{d}p_0}{\mathrm{d}r} = -\frac{G\mathscr{M}}{r^n}. \tag{8}$$

4. Conditions at the ionization front

The narrow region, in which the neutral gas becomes ionized, i.e. where absorption of radiation from the star is intense, is represented mathematically as a discontinuity, which is termed an ionization front. Suffixes i and n are used to denote data on the ionized and neutral sides of the front. Then, provided that there is not sufficient time for the ionized gas to recombine on passage through the front, it can be shown from ionization balance, mass, momentum and energy considerations that

$$J_i = \frac{\rho_n x_i}{M}(U_i - u_n), \tag{9}$$

$$\rho_i(U_i - u_i) = \rho_n(U_i - u_n), \tag{10}$$

$$p_i + \rho_i(U_i - u_i)^2 = p_n + \rho_n(U_i - u_n)^2, \tag{11}$$

$$\frac{5}{2}\frac{p_i}{\rho_i} + \tfrac{1}{2}(U_i - u_i)^2 = \frac{5}{2}\frac{p_n}{\rho_n} + \tfrac{1}{2}(U_i - u_n)^2 + \tfrac{1}{2}x_i Q_0^2, \tag{12}$$

where U_i is the velocity of the front defined by $r = R_i(t)$. These equations were obtained and discussed by Kahn (1954) for the case when $x_i = 1$.

5. Form of the solution

In an attempt to solve the rather complicated partial differential equations in §2 subject to the given boundary conditions, several difficulties were immediately apparent. Among them was that of knowing the initial flow pattern. For instance, it is not known whether a

shock in addition to the ionization front will occur in the neutral gas or perhaps even in the ionized region, and the difficulty of solving partial differential equations without this information is well known. We will therefore look for a similarity solution depending on one independent variable only, so that the system of partial differential equations will reduce to a system of ordinary differential equations. For the similarity solution to be applicable the size of the star must no longer be a relevant factor in determining the motion of the gas. The star has thus to be regarded as a point or line source of radiation, with a total photon output equal to that of the star, thus

$$\lim_{r\to 0} Jr^n = J_* R_*^n. \tag{13}$$

Several restrictions are immediately placed upon the form of the similarity solution.

(i) The surface temperature T_* of the star is constant; moreover, the spectral quality of the radiation field has been assumed to be constant also, so that Q_0, which is a typical velocity in the problem, is constant. Hence the similarity variable η must be proportional to t/r. The solution can therefore only be applied to problems where the ionized region expands at a constant rate.

(ii) Equation (9) and restriction (i) require that J/ρ must remain a constant at the ionization front; hence J/ρ must be a function of η only.

(iii) Jr^n must be a function of η only so that Jr^n will tend to a finite limit as $r \to 0$ (i.e. $\eta \to \infty$).

We are now in a position to write down the similarity forms allowed:

$$\left.\begin{aligned} u = \frac{r}{t}\mathscr{U}(\eta), \quad p = \frac{1}{r^n}\left(\frac{r}{t}\right)^2 \mathscr{P}(\eta), \quad \rho = \frac{1}{r^n}\omega(\eta), \\ T = T(\eta), \quad x = x(\eta), \quad J = \frac{1}{r^n}\mathscr{J}(\eta), \end{aligned}\right\} \tag{14}$$

where $\eta = (t/r)\sqrt{(2kT_c/M)}$ and T_c is a temperature to be defined later. It is also convenient to introduce the speed of sound

$$a = \frac{r}{t}\mathscr{A}(\eta) = \sqrt{\frac{5}{3}}\frac{r}{t}\frac{\mathscr{P}(\eta)}{\omega(\eta)}. \tag{15}$$

6. Spherical ionization fronts (recombination in H II region neglected)

The form of the similarity solution in the spherically symmetric problem requires the initial density ρ_0 in the neutral gas to vary as

$$\rho_0 = \omega_0 r^{-2}, \tag{16}$$

where ω_0 is some constant parameter. For the gas to be in equilibrium equation (8) reveals that the pressure in the undisturbed gas must vary as

$$p_0 = G\mathscr{M}\omega_0/3r^3 + \text{constant}. \tag{17}$$

This is at variance with the similarity form assumed for the pressure. In order to overcome this difficulty we assume that the pressure p_0 in front of the ionization front, or the shock wave, if one occurs, can be ignored in comparison with the pressure behind; the form for p_0 is then arbitrary. In all the cases which will be considered this will prove to be true.

Substituting the similarity forms into the equations of motion, we find that they can only be possible solutions if recombination in the H II region is neglected and the gas is fully

ionized. Gravitational forces in the H II region and the cooling caused by the excitation of O^+ ions have also to be ignored. Equations (4) to (6) then reduce to the Euler equations for ideal fluid flow; to these we add

$$Jr^2 = J_* R_*^2 \quad \text{and} \quad x = 1. \tag{18}$$

Although by making these approximations we neglect many interesting features that one would like to include, it is hoped that a solution based upon them will point out their limitations in regard to applicability. Several authors have made similar approximations in other related problems. A more detailed treatment will be given later and comparison can then be made. Inserting expressions (14) and (15) into the reduced equations of motion, we obtain after a certain amount of manipulation,

$$D\eta \frac{\mathrm{d}\mathscr{U}}{\mathrm{d}\eta} = (1-\mathscr{U})^2 \mathscr{U} - 3[\mathscr{U} - \tfrac{2}{5}]\mathscr{A}^2, \tag{19}$$

$$\frac{D\eta}{\mathscr{A}} \frac{\mathrm{d}\mathscr{A}}{\mathrm{d}\eta} = \frac{(3-5\mathscr{U})\,[5(1-\mathscr{U})^2 - 3\mathscr{A}^2]}{15(1-\mathscr{U})}, \tag{20}$$

$$\frac{D\eta}{\omega} \frac{\mathrm{d}\omega}{\mathrm{d}\eta} = \frac{2\mathscr{A}^2(3-5\mathscr{U})}{5(1-\mathscr{U})}, \tag{21}$$

with $D = (1-\mathscr{U})^2 - \mathscr{A}^2$.

By dividing equation (20) by equation (19) we obtain the differential equation

$$\frac{\mathrm{d}\mathscr{A}}{\mathrm{d}\mathscr{U}} = \frac{\mathscr{A}(3-5\mathscr{U})\,[5(1-\mathscr{U})^2 - 3\mathscr{A}^2]}{3(1-\mathscr{U})\,[5\mathscr{U}(1-\mathscr{U})^2 - 3\mathscr{A}^2(5\mathscr{U}-2)]}, \tag{22}$$

which can be solved numerically. Once this has been done η and ω can be determined from equations (19) and (21). The behaviour of the solutions of equation (22) is shown in figure 1. Each integral curve corresponds to a certain value of the arbitrary constant involved in the integration of equation (22). The arrows marked in the figure indicate the direction of increasing η, i.e. of decreasing r for fixed time. On crossing the 'critical' lines $|1-\mathscr{U}| = |\mathscr{A}|$ the direction is reversed. Thus no integral curve crossing these lines can represent a real flow, since for a given value of η there would correspond two possible values of the fluid velocity.

Substituting expressions (14) and (15) in the ionization front relations (9) to (12), we obtain

$$MJ_i R_i^2 = MJ_* R_*^2 = U_i(1-\mathscr{U}_n)\,\omega_n, \tag{23}$$

$$\omega_i(1-\mathscr{U}_i) = \omega_n(1-\mathscr{U}_n), \tag{24}$$

$$\frac{3\mathscr{A}_i^2}{1-\mathscr{U}_i} - 5\mathscr{U}_i = \frac{3\mathscr{A}_n^2}{1-\mathscr{U}_n} - 5\mathscr{U}_n, \tag{25}$$

$$3\mathscr{A}_i^2 + (1-\mathscr{U}_i)^2 = 3\mathscr{A}_n^2 + (1-\mathscr{U}_n)^2 + (Q_0/U_i)^2. \tag{26}$$

We first consider the conditions under which an ionization front moves into the neutral gas without a shock wave developing ahead of it. For this case $\mathscr{U}_n = 0$, $\omega_n = \omega_0$ and we assume $\mathscr{A}_i \gg \mathscr{A}_n$, i.e. $p_i \gg p_0$. The ionization front will be R type. Equation (25) then becomes

$$\mathscr{A}_i^2 = \tfrac{5}{3}(1-\mathscr{U}_i)\,\mathscr{U}_i, \tag{27}$$

which, on substituting into equation (26), gives

$$U_i^2 = \frac{Q_0^2}{\mathscr{U}_i(3-4\mathscr{U}_i)}. \tag{28}$$

Also, from equation (23) and (28), we obtain

$$\omega_0 = \sqrt{\{\mathscr{U}_i(3-4\mathscr{U}_i)\}}\, MJ_* R_*^2 Q_0^{-1}. \tag{29}$$

We now require the value of $\mathscr{U}_i$. Relation (27) imposes the condition that $\mathscr{U}_i < \frac{3}{4}$ so that only a section of the curve determined by equation (27), represents states which may exist behind an R-type ionization front. The curve is shown in figure 1 and bears the label 'R i.f.' curve. We now follow in the direction of increasing η any integral curve of equation (22) which cuts this R i.f. curve. It will be observed that all integral curves except one cross

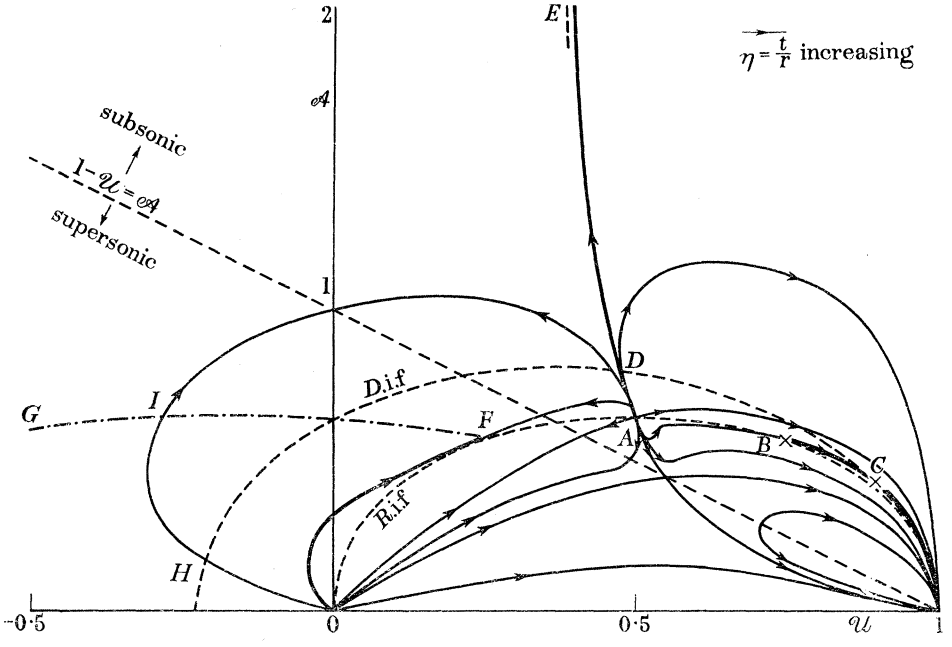

FIGURE 1. The $(\mathscr{U},\mathscr{A})$-plane representing solutions of the differential equation (22).

the critical line or enter the singularity $\mathscr{U}=1, \mathscr{A}=0$. If the star is assumed to be at rest, the curves entering this singular point $(1,0)$ can be disregarded. The curve ADE in figure 1 is the exception. It has the property that $\mathscr{U}$ is asymptotic to $2/5$ as $\mathscr{A}$ approaches infinity. Use of equation (19) shows that as $\mathscr{A} \to \infty$ along this integral curve r/t tends to zero, which means that the fluid is at rest at the centre, i.e. at the star, and this is what we require. But the integral curve also passes through the singular point $A\{\mathscr{U}=\frac{1}{2}, \mathscr{A}=\sqrt{(\frac{5}{12})}\}$, which is on the R i.f. curve. It can easily be verified that on approaching this singularity r/t tends to infinity, which would mean that the ionization front travelled with infinite speed. This is not the case, and it is therefore necessary to look for another solution. This turns out to be the 'trivial' solution of equation (19), when both the numerator and denominator are identically zero, namely

$$\mathscr{U} = \tfrac{1}{2}, \quad \mathscr{A} = \sqrt{(\tfrac{5}{12})}. \tag{30}$$

Thus

$$u = \frac{1}{2}\frac{r}{t}, \quad a = \sqrt{\frac{5}{12}}\frac{r}{t}. \tag{31}$$

Substituting these values in (28) and (29) we find that the ionization front moves with a speed

$$U_i = \sqrt{2}\, Q_0, \tag{32}$$

and that the assumed flow pattern, i.e. no shock ahead of the ionization front, is correct provided that the initial density distribution is such that ω_0 is given by

$$\omega_0 = 2^{-\frac{1}{2}} M J_* R_*^2 Q_0^{-1}. \tag{33}$$

The variation of $J_* R_*^2$ and Q_0 for differing types of stars is shown in table 1, which is taken from Kahn (1954). The ionization front in this case moves with supersonic speed relative to the fluid ahead and subsonic speed relative to fluid behind, i.e. strong R-type similar to a strong detonation.

We now consider the case when a strong shock moves ahead of an ionization front, thus disturbing the neutral gas before ionization takes place. The differential equations to be solved in the disturbed neutral gas are similar to those used in the H II region, though it must be remembered that in the H I region $x = 0$. A strong shock is represented in the $(\mathscr{U},\mathscr{A})$-plane by the point $B(\frac{3}{4}, \frac{1}{4}\sqrt{5})$. From B we follow the integral curve in the direction of η increasing to some point C, say, which determines U_n and $\mathscr{A}_n$. By substituting these values in equation (25) we obtain a relation between $\mathscr{U}_i$ and $\mathscr{A}_i$; this is plotted in figure 1 and bears the label 'D i.f.' curve, the 'D' indicating that the ionization front in this case is D-type. If we now consider all the integral curves, which cross the D i.f. curve, the integral curve

TABLE 1

type of star	$O5$	$O7$	$O9$	$B0$	$B2$
$J_* R_*^2$ (s^{-1})	$1{\cdot}2 \times 10^{50}$	$4{\cdot}7 \times 10^{48}$	$2{\cdot}9 \times 10^{47}$	$1{\cdot}4 \times 10^{46}$	$1{\cdot}2 \times 10^{45}$
Q_0 (cm s^{-1})	$3{\cdot}6 \times 10^{6}$	$2{\cdot}9 \times 10^{6}$	$2{\cdot}3 \times 10^{6}$	$2{\cdot}1 \times 10^{6}$	$1{\cdot}8 \times 10^{6}$

DE yields a solution with the star at rest at the centre. Thus the required solution $\mathscr{A}(\mathscr{U})$ of equation (22) in this case is made up of the sections BC and DE continued to $\mathscr{A} = \infty$, the sections representing the flow set up in the neutral and ionized gases, respectively. By substituting $\mathscr{A}(\mathscr{U})$ in equations (19) and (21) we obtain η/η_i and ω/ω_0 as functions of $\mathscr{U}$. The corresponding values of ω_0 and U_i are then determined from equations (23) and (26). By varying the point C we can obtain corresponding values of $(\omega_0 Q_0)/(MJ_* R_*^2)$ and U_i/Q_0 for which a shock wave will propagate with speed U_s ahead of the ionization front. This relation and the corresponding values of U_i/U_s are shown plotted in figure 2.

Figure 2 shows that $\omega_0 \geqslant MJ_* R_*^2/Q_0\sqrt{2}$, $0{\cdot}84 \leqslant U_i/U_s \leqslant 1$ in the range $0 \leqslant U_i/\sqrt{2}\,Q_0 \leqslant 1$. Thus even in the extreme case when ω_0 is large figure 2 shows that the velocity of the shock relative to the ionization front is small; this suggests that the neutral gas will be compressed in a narrow shell outside the expanding H II region. Some typical values of ω_0, the speed of the ionization front, the temperature T_i behind the ionization front and the temperature T_s behind the shock are given in table 2 for the case when a strong ionization front travels by itself, and for a particular case when compression by a strong shock precedes ionization. From figure 1 it will be observed that the ionization front, for the case when a shock wave propagates ahead of it, moves with subsonic speed relative to the fluid both ahead and behind the front. (The points C and D both lie in the subsonic region.) The ionization front therefore corresponds to a weak D-type front similar to a weak deflagration. The extreme case of a strong ionization front (strong R-type) could have been regarded as a combination of a D-type front and a strong shock wave propagating at the same speed, as both figures 1 and 2 indicate.

PHILOSOPHICAL TRANSACTIONS OF THE ROYAL SOCIETY A MATHEMATICAL, PHYSICAL & ENGINEERING SCIENCES

For the case $\omega_0 < (MJ_* R_*^2)/(Q_0\sqrt{2})$ an understanding of the flow pattern is not too clear. An examination of figure 1 rules out the possibility of an ionization front moving without the presence of a shock wave, except for the particular case already described. The only other flow pattern which is mathematically possible takes into account the possibility of a shock wave developing inside the ionized region. This shock wave will have to be such that conditions behind the shock are described by a point on the integral curve AE (so that the fluid will be at rest at the centre). Thus the possible flow immediately ahead of such a shock can be computed and in figure 1 this is represented by the curve FG. If we follow a typical integral curve from any point of FG in the direction η decreasing, it enters the singularity at

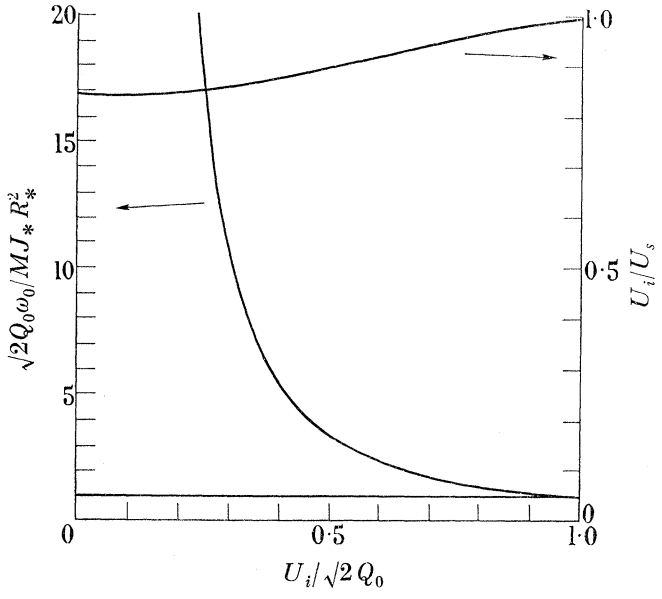

FIGURE 2. $\sqrt{2Q_0\omega_0}/MJ_* R_*^2$ and U_i/U_s shown as a function of $U_i/\sqrt{2Q_0}$.

TABLE 2

type of star	ω_0	U_i(km/s)	T_i(°K)	T_s(°K)
$O5$	$0{\cdot}4 \times 10^{20}$	50	475 00	—
$B2$	$0{\cdot}8 \times 10^{15}$	25	12 000	—
$O5$	$1{\cdot}1 \times 10^{20}$	28	24 700	26 800
$B2$	$2{\cdot}2 \times 10^{15}$	14	6250	6700

the origin without crossing the R i.f. curve. It does, however, cross the D i.f. curve hence, if the pattern represented a possible flow in the ionized region, a shock wave with a D-type ionization front following it must occur. We thus follow the procedure described in the previous paragraph; start at the strong shock point B, move from B along the integral curve to some point C, say, then fit a D-type ionization front in, behind which the flow is represented by some point on the D i.f. curve, say H, in the region bounded by the curve FG, the negative U-axis and the curve FO which is the integral curve of equation (22) through F. Now follow the curve HI until the point I of the curve FG is reached. At this point a shock occurs, where the flow variables change discontinuously to conditions represented by the point D, from thence we proceed to the star along the integral curve DE. It is interesting to note that the ionization front in this case is a strong D-type (similar to a strong deflagration wave). The question, which obviously comes to mind, is whether a strong D-type ionization front can exist? Such a question can only be answered by a discussion of the ionization front

structure. Another difficulty also appears for the case described in this paragraph, for it is found that there is not a unique solution—any point of the D i.f. curve in the region bounded by $GIFO$ and the negative U-axis could have been chosen. The question of uniqueness and whether strong D-type ionization fronts occur is answered by Axford in the following paper which deals with their structure. It is shown there that if recombination and cooling is neglected then strong D-type fronts are not possible. Thus what happens when $\omega_0 < (MJ_* R_*^2)/Q_0\sqrt{2}$ is still an open question.

However, there are other features of the results of this section that are equally disturbing. In figure 3 the distribution of density, pressure, velocity and temperature of the gas is

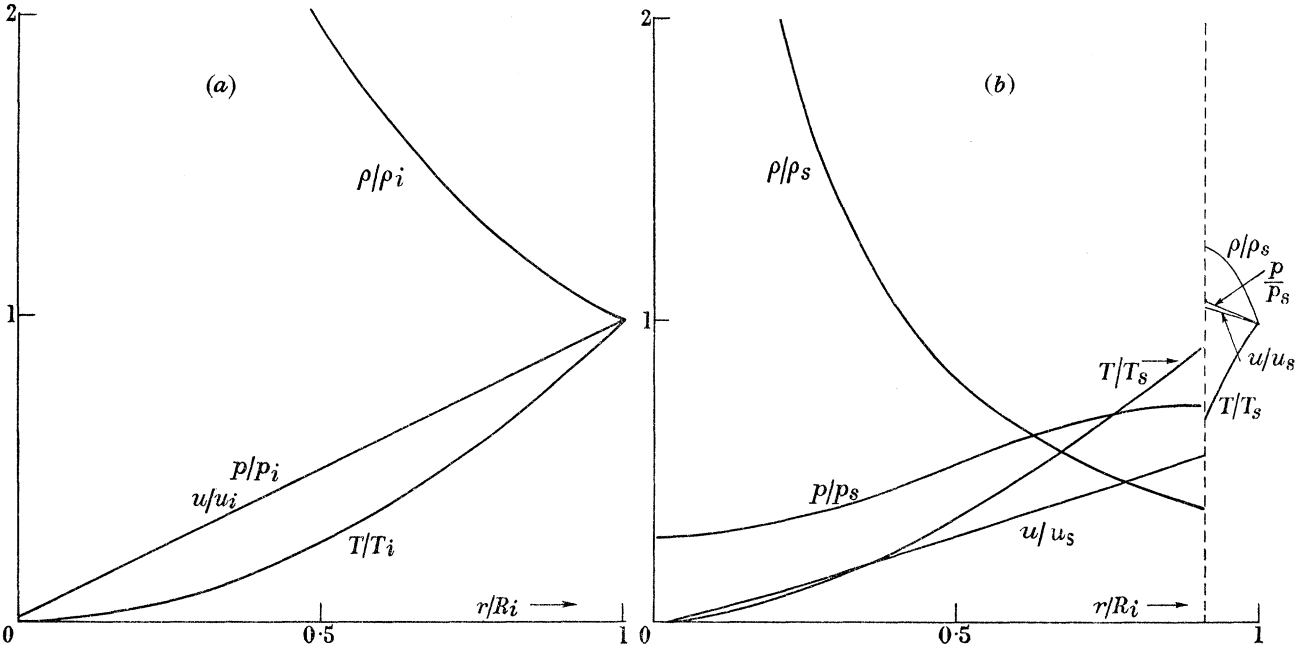

FIGURE 3. Temperature, density, pressure and gas-velocity distributions for cases (a) ionization front only, (b) ionization front with shock ahead.

plotted for the two cases for which the parameters have been given in table 2. One notices from table 2 and figure 3 immediately that behind the ionization front the temperature is large while at the centre the temperature goes to zero! This is the outcome of neglecting recombination and any subsequent re-ionization of the recombined atoms by absorption of radiation from the star. The combined effect of these two processes would be to maintain the temperature at a finite value.

Thus to obtain a better picture of the flow we need to consider the effect of the recombination of ions with electrons.

7. CYLINDRICAL IONIZATION FRONTS (INCLUDING THE EFFECT OF RECOMBINATION, ETC.)

For mathematical reasons a complete solution of equations (1) to (6) can best be obtained for a problem in which cylindrical symmetry exists. Though such a solution obviously is restricted in its physical application, it will, however, serve as an indication to what happens in the real case. We consider a 'cylindrical' star model, which is made up of a group of stars of the same type uniformly distributed along a line at a distance d apart, with a total photon output equal to the sum of the outputs of the individual stars. The photon output

per unit length of cylinder can then be approximately related to the output from each individual spherical star by the equation,

$$(J_* R_*)_{\text{cyl.}} = (2/d)\,(J_* R_*^2)_{\text{sph.}} \tag{34}$$

For the cylindrical case $n = 1$, so that for a similarity solution, the initial distribution of density must be given by $\rho_0 = \omega_0 r^{-1}$. This variation is compatible with equation (8) if the neutral gas is at a uniform temperature T_0 and $G\mathscr{M}M/kT_0 = 1$. When numerical values are inserted, $\mathscr{M}$, which is twice the mass of the 'cylindrical' star per unit length, is found to be $12 \times 10^{14} T_0$ g/cm. Since this is a rather special value it is better to neglect gravitation as was done in the spherical case. We will, however, use it to estimate particular values of d, which up to now has been completely arbitrary. In a similar way to that used in relating photon outputs, we relate the mass per unit length of cylinder to the mass of each individual star. Substituting $T_0 = 100$ °K, we find the values of d shown in table 3. This enables a comparison to be made between cylindrical and spherical models.

TABLE 3

type of star	$O5$	$O7$	$O9$	$B0$	$B2$
$10^{-16} d$ (cm)	48	32	16	8	4

By substituting the appropriate similarity expressions (14) and (15) in equations (1) to (6), five ordinary differential equations are obtained. These can be rearranged to give the following set of equations,

$$D\eta \frac{\mathrm{d}\mathscr{U}}{\mathrm{d}\eta} = \mathscr{U}(1-\mathscr{U})^2 + \{\tfrac{3}{5} - 2\mathscr{U} + \tfrac{2}{5}F\}\mathscr{A}^2, \tag{35}$$

$$\frac{D\eta}{\mathscr{A}}\frac{\mathrm{d}\mathscr{A}}{\mathrm{d}\eta} = \frac{1}{3(1-\mathscr{U})}\left[(3-4\mathscr{U})\,(1-\mathscr{U})^2 - 3(\tfrac{4}{5}-\mathscr{U})\mathscr{A}^2 + \{(1-\mathscr{U})^2 - \tfrac{3}{5}\mathscr{A}^2\}F\right], \tag{36}$$

$$\frac{D\eta}{\omega}\frac{\mathrm{d}\omega}{\mathrm{d}\eta} = \frac{\mathscr{A}^2}{1-\mathscr{U}}\left[\tfrac{3}{5} - \mathscr{U} + \tfrac{2}{5}F\right], \tag{37}$$

$$(1-\mathscr{U})\frac{\mathrm{d}x}{\mathrm{d}\eta} = \alpha\sqrt{\left(\frac{M}{2kT_c}\right)}\left[\mathscr{J}(1-x) - \frac{3\times 10^{-10}}{\alpha M}\frac{\omega x^2}{T^{\frac{3}{4}}}\right], \tag{38}$$

$$\eta\frac{\mathrm{d}\mathscr{J}}{\mathrm{d}\eta} = \frac{\alpha}{M}\mathscr{J}\omega(1-x), \tag{39}$$

where

$$D = (1-\mathscr{U})^2 - \mathscr{A}^2, \tag{40}$$

$$\mathscr{A}^2 = \tfrac{5}{6}(1+x)\,\eta^2(T/T_c), \tag{41}$$

$$F = \frac{5}{3}\left(\frac{M}{2kT_c}\right)^{\frac{3}{2}}\frac{\eta^3}{\mathscr{A}^2}\left[\frac{\alpha}{2}\mathscr{J}(1-x)\,Q_0^2 - \frac{3\times 10^{-10}}{M^2}\frac{x^2\omega}{T^{\frac{3}{4}}}\tfrac{3}{2}kT - \frac{\omega x^2}{M^2}L_{ei}(T)\right] \tag{42}$$

and T_c is a temperature to be defined later.

Equations (35) to (39) should now be solved starting with an asymptotic series for the dependent variables as $\eta \to \infty$. The series can be shown to be of the form

$$\left.\begin{aligned} &\mathscr{U} \sim \tfrac{1}{2} + \frac{\mu_1}{\eta} + \ldots, \quad \mathscr{A}^2 \sim \eta^2\left(\zeta_0 + \frac{\zeta_1}{\eta} + \ldots\right), \quad \omega \sim \frac{1}{\eta}\left(\Omega_0 + \frac{\Omega_1}{\eta} + \ldots\right), \\ &x \sim 1 - \frac{\gamma_1}{\eta} + \ldots, \quad \mathscr{J} \sim \mathscr{J}_* + \frac{1}{\eta^2}\left(\delta_0 + \frac{\delta_1}{\eta} + \ldots\right), \\ &F \sim 1 + \frac{\nu_1}{\eta} + \ldots, \quad T \sim \theta_0 + \frac{\theta_1}{\eta} + \ldots, \end{aligned}\right\} \tag{43}$$

where μ_1, ζ_0, ζ_1, Ω_0, Ω_1, γ_1, δ_0, δ_1, ν_1, θ_0, θ_1, etc., are constants related to each other. Substituting the series (43) in equations (38), (41) and (42) and equating terms of largest order, we obtain

$$\mathscr{I}_* \gamma_1 = \frac{3\times 10^{-10}}{\alpha M}\frac{\Omega_0}{\theta_0^{\frac{3}{4}}}, \tag{44}$$

$$\zeta_0 = \frac{5}{3}\frac{\theta_0}{T_c}, \tag{45}$$

$$1 = \left(\frac{M}{2kT_c}\right)^{\frac{3}{2}}\frac{T_c}{\theta_0}\left[\frac{\alpha}{2}\mathscr{I}_*\gamma_1 Q_0^2 - \frac{3\times 10^{-10}}{M^2}\frac{\Omega_0}{\theta_0^{\frac{3}{4}}}\tfrac{3}{2}k\theta_0 - \frac{\Omega_0}{M^2}L_{ei}(\theta_0)\right]. \tag{46}$$

Eliminating $\mathscr{I}_*\gamma_1$ from equations (44) and (46), and putting $Q_0^2 = 2kT_*/M$, we obtain

$$1 = 0{\cdot}9\times 10^{14}\left(\frac{M}{2kT_c}\right)^{\frac{1}{2}}\frac{\Omega_0}{\theta_0^{\frac{3}{4}}}\left[\frac{T_*}{\theta_0} - \frac{3}{2} - 2{\cdot}4\times 10^{25}\theta_0^{-\frac{1}{4}}L_{ei}(\theta_0)\right], \tag{47}$$

TABLE 4

type of star	$O5$	$O7$	$O9$	$B0$	$B2$
T_*(°K)	80000	50000	32000	25000	20000
T_c(°K)	9420	8290	7360	6880	6470

which is an equation determining, in terms of Ω_0 and T_c, the temperature of the ionized gas near the radiating star. Assuming θ_0 to be of the order of 10000 °K and $(M/2kT_c)^{\frac{1}{2}}\Omega_0 \ll 10^{11}$, then θ_0 is approximately given by

$$\frac{T_*}{\theta_0} - \tfrac{3}{2} - 2{\cdot}4\times 10^{25}\theta_0^{-\frac{1}{4}}L_{ei}(\theta_0) = 0. \tag{48}$$

We will denote this value of θ_0 by T_c and it is shown tabulated in table 4 for differing values of T_*. Other equations may be obtained which connect the various constants in the series expansions. However, if one pursues this method further there does arise the difficulty of matching conditions at the centre to conditions in the undisturbed H I region, i.e. relating the values of the parameters ω_0 and T_* to the constants in the series expansions. It turns out that a series of test runs must be made on a computing machine before the required information is obtained.

One can, however, derive an extremely accurate result without much labour. The basic approximation involved does not require the introduction of similarity into the problem at all, and the approximation holds also in the spherical and plane cases. Eliminate J between equations (2) and (6) and use the continuity equation (5) to obtain

$$\frac{\mathrm{D}}{\mathrm{D}t}\left(\frac{3}{2}\frac{p}{\rho}\right) + p\frac{\mathrm{D}}{\mathrm{D}t}\left(\frac{1}{\rho}\right) - \frac{Q_0^2}{2}\frac{\mathrm{D}x}{\mathrm{D}t} = \frac{\beta\rho x^2}{M}\left(\frac{Q_0^2}{2} - \frac{3}{2}\frac{kT}{M}\right) - \frac{\rho x^2}{M}L_{ei}(T). \tag{49}$$

By using equation (3) and substituting for β, this can be rewritten

$$\frac{3}{2T}\frac{\mathrm{D}T}{\mathrm{D}t} - \frac{1}{\rho}\frac{\mathrm{D}\rho}{\mathrm{D}t} - \left(\frac{MQ_0^2}{2kT} - \frac{3}{2}\right)\frac{1}{1+x}\frac{\mathrm{D}x}{\mathrm{D}t}$$
$$= \frac{1{\cdot}8\times 10^{14}\rho x^2}{(1+x)\,T^{\frac{3}{4}}}\left[\frac{MQ_0^2}{2kT} - \frac{3}{2} - 2{\cdot}4\times 10^{25}T^{-\frac{1}{4}}L_{ei}(T)\right]. \tag{50}$$

If we take a time-scale of a million years, so that t is expressed in terms of this quantity as unit, the right-hand sides must be multiplied by 3×10^{13} and the numerical coefficient

becomes 1×10^{27}. Hence, even with densities of a few hydrogen atoms per cubic centimetre the quantity inside the square brackets on the right-hand side of equation (50) is multiplied by a very large factor. Thus, unless T is near the value T_c, for which the quantity in the square brackets is zero, at least one term on the left-hand side of equation (50) must be large. We rule out a large rate of change of x and ρ, and consider the rate of change of the temperature. Approximately, we can write

$$\frac{3}{2T}\frac{\mathrm{D}T}{\mathrm{D}t} \simeq \frac{1{\cdot}8\times10^{14}\rho x^2}{(1+x)\,T^{\frac{3}{4}}}\left[\frac{MQ_0^2}{2kT}-\frac{3}{2}-2{\cdot}4\times10^{25}T^{-\frac{1}{4}}L_{ei}(T)\right]. \tag{51}$$

Thus, if $T \lesseqgtr T_c$ then $\mathrm{D}T/\mathrm{D}t \gtreqless 0$, i.e. if at any point of the ionized region the temperature is different from T_c then it will increase or decrease to it in a short interval of time. To see this more clearly put $T = T_c + T'$ and assume T' to be a small perturbation, equation (51) approximates to

$$\frac{1}{T'}\frac{\mathrm{D}T'}{\mathrm{D}t} \simeq \frac{2}{3}\frac{1{\cdot}8\times10^{14}\rho x^2}{(1+x)\,T_c^{\frac{3}{4}}}\left[\frac{MQ_0^2}{2kT_c}-0{\cdot}6\times10^{25}T_c^{-\frac{1}{4}}L_{ei}(T_c)+2{\cdot}4\times10^{25}T_c^{\frac{3}{4}}\left(\frac{\mathrm{d}L_{ei}}{\mathrm{d}T}\right)_{T=T_c}\right]. \tag{52}$$

For $T_c = 10\,000\ ^\circ\mathrm{K}$ the time interval would be of the order of $\rho^{-1}10^{-12}$ s. If $\rho = 10^{-23}$ g/cm^3, the time interval is about 6000 years, which is small compared to the time scale involved in the problem. The cooling and the subsequent re-ionization of recombined atoms therefore maintain the ionized gas at a constant temperature T_c, so that we can with confidence replace the energy equation (6) by $T = T_c$. The analysis can be simplified further, for in the H II region the gas will be nearly fully ionized, so that x can be assumed approximately equal to 1 and $\mathrm{D}x/\mathrm{D}t$ can be neglected in equation (2), i.e. a balance is assumed to take place between ionization and recombination. Using the equation of continuity (5), equation (2) then becomes

$$\alpha J(1-x) = \beta\rho/M. \tag{53}$$

The reader should note that it is necessary to retain the variation of $(1-x)$ in the absorption term since J is large.

When the above approximations are made the equations of energy across the ionization front must also be modified. We must now allow for the rapid cooling of the gas by recombination and the excitation of O^+ ions in the region of the ionization front, so that a particle of fluid having passed through the front is almost at once at a temperature T_c. This means that only the equations of continuity (10) and momentum (11) of the ionization front relations are valid. These turn out to be sufficient to solve the problem.

We will now use the foregoing approximations to determine the flow when the initial distribution is given by $\rho_0 = \omega_0 r^{-1}$. Substituting $T = T_c$, $x = 1$ and the similarity forms (14) and (15) into equations (3), (4) (with gravity neglected) and (5) we obtain

$$D_1\eta\frac{\mathrm{d}\mathscr{U}}{\mathrm{d}\eta} = \mathscr{U}(1-\mathscr{U})^2+(1-2\mathscr{U})\,\eta^2, \tag{54}$$

$$\frac{D_1}{\omega}\frac{\mathrm{d}\omega}{\mathrm{d}\eta} = \eta, \tag{55}$$

where $D_1 = (1-\mathscr{U})^2-\eta^2$. These equations could have been obtained from equations (35) to (37) by substituting in equation (36)

$$\mathscr{A} = \sqrt{\tfrac{5}{3}}\,\eta, \tag{56}$$

thus obtaining
$$F = \frac{\mathscr{U}(1-\mathscr{U})^2-\eta^2}{(1-\mathscr{U})^2-\eta^2}. \tag{57}$$

Also by putting $x \doteq 1$ in equation (38) and (39) we obtain

$$\alpha \mathscr{J}(1-x) = \frac{3\times 10^{-10}}{MT_c^{\frac{3}{4}}}\omega, \tag{58}$$

and
$$\eta \frac{\mathrm{d}\mathscr{J}}{\mathrm{d}\eta} = \frac{3\times 10^{-10}}{M^2T_c^{\frac{3}{4}}}\omega^2, \tag{59}$$

so that once ω has been determined x and $\mathscr{J}$ can be calculated from equations (58) and (59).

If the neutral gas is disturbed before it is ionized then we must also solve the equations obtained by substituting the similarity expressions (14) and (15) in the equations appropriate to the non-ionized gas; this yields the following set of equations.

$$D\eta \frac{\mathrm{d}\mathscr{U}}{\mathrm{d}\eta} = \mathscr{U}(1-\mathscr{U})^2+\mathscr{A}^2(\tfrac{3}{5}-2\mathscr{U}), \tag{60}$$

$$\frac{D\eta}{\mathscr{A}}\frac{\mathrm{d}\mathscr{A}}{\mathrm{d}\eta} = \frac{1}{3(1-\mathscr{U})}[(3-4\mathscr{U})(1-\mathscr{U})^2+\mathscr{A}^2(\tfrac{3}{5}-2\mathscr{U})], \tag{61}$$

$$\frac{D\eta}{\omega}\frac{\mathrm{d}\omega}{\mathrm{d}\eta} = \frac{(\frac{3}{5}-\mathscr{U})\mathscr{A}^2}{1-\mathscr{U}}, \tag{62}$$

where $D = (1-\mathscr{U})^2-\mathscr{A}^2$.

Since equations (60) and (61) are best solved by working in the $(\mathscr{U},\mathscr{A})$-plane, we also solve equation (54) in that plane using equation (56). In a similar manner to that described in § 6 we can discuss the integral curves in the $(\mathscr{U},\mathscr{A})$-plane. The significant curves are shown in figure 4. The curve BCM is an integral curve representing a solution in $(\mathscr{U},\mathscr{A})$-plane of equations (60) and (61) with η eliminated, the other curves represent solutions of the differential equation (54).

The curve marked Ri.f. represents possible states behind a R-type ionization front (there is no restriction on $\mathscr{U}$ since equation (26) is now no longer applicable).

We first consider the case when an ionization front travels by itself. The ionization front in this case is strong R-type and corresponds in figure 4 to the point A. The solution in the H II region is represented by the integral curve ADE through A followed in the direction η increasing; it has the property that as $\eta \to \infty$, $\mathscr{U} \to \frac{1}{2}$. The speed of the ionization front is calculated from the computed value of $\mathscr{A}_i(=\sqrt{\frac{5}{3}}\eta_i)$ and is found to be given by

$$U_i = \sqrt{(2kT_c/0{\cdot}23M)}. \tag{63}$$

It is interesting to note that for this value of U_i the absolute velocity of the gas behind the front is approximately sonic. By integrating equation (55) along the integral curve ADE continued to infinity, we can obtain ω/ω_0. Similarly we can determine from equations (58) and (59) the values of $\mathscr{J}(1-x)/\omega_0$ and $(\mathscr{J}-\mathscr{J}_*)/\omega_0^2$ at the front. In order to find $\mathscr{J}$ and $(1-x)$ explicitly we need to know the value of ω_0. This can be found by investigating the internal structure of an ionization front, but since this is rather complicated it is better to approximate as follows. To find the order of magnitude of $\mathscr{J}_i$, let us assume that it is of the same order as the number of photons which would have been required to propagate an

ionization front with speed U_i in an undisturbed gas of density variation $\rho_0(r) = \omega_0/r$ assuming that no recombination takes place at the front. From equation (23) we see that

$$\mathscr{J}_i = O\left(\frac{U_i\omega_0}{M}\right). \tag{64}$$

Thus if $\omega_0 \ll (M\mathscr{J}_*)/U_i$, then $\mathscr{J}_i \ll \mathscr{J}_*$. Assuming this to be true, the value of ω_0 can be determined since $-\mathscr{J}_*/\omega_0^2$ and $\mathscr{J}_*$ are known. Axford's results which deal with the structure of an ionization front bear out the validity of these approximations. Physically they amount to saying that, in order that the temperature may be maintained at a value

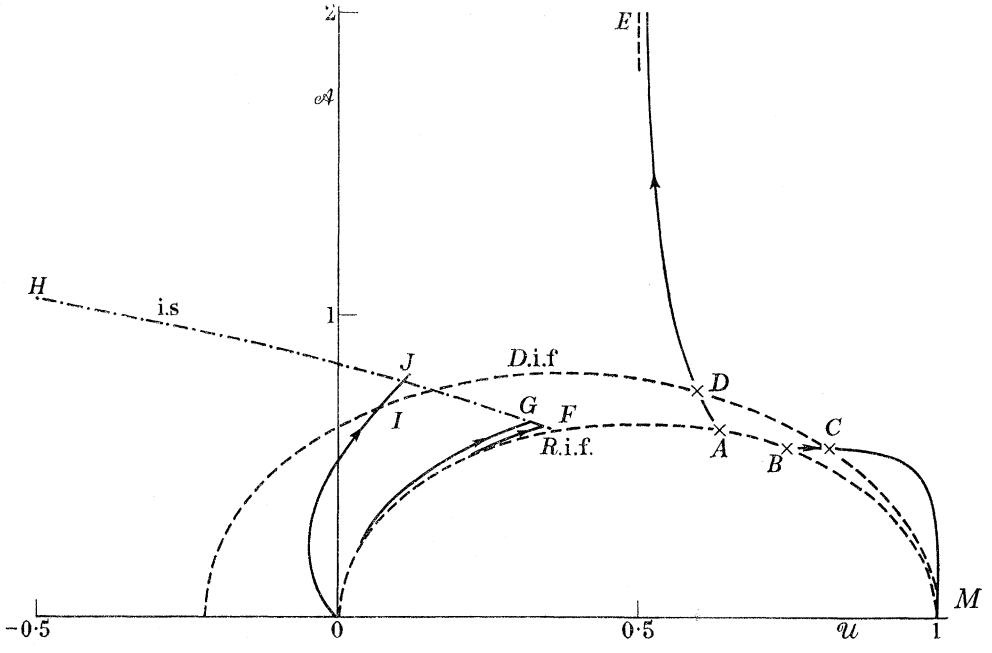

FIGURE 4. The $(\mathscr{U},\mathscr{A})$-plane representing the solutions of the differential equations (54), and (60) and (61) combined.

T_c, an appreciable part of the star's radiation must be absorbed within the ionized region. From equations (1) and (2), and assuming $\mathscr{J}_i \ll \mathscr{J}_*$, an approximate relationship between $\mathscr{J}_*$ and ω_0 is obtained, namely

$$\mathscr{J}_* = J_* R_* \simeq \frac{\beta}{M^2}\int_0^{R_i} \rho^2 r\,\mathrm{d}r = \frac{3\times 10^{-10}\omega_0^2}{T_c^{\frac{3}{4}} M^2}\int_\infty^{\eta_i} \frac{(\omega/\omega_0)^2}{\eta}\,\mathrm{d}\eta. \tag{65}$$

Substituting the numerical value of the integral in equation (65) one finds that

$$\omega_0 = 0{\cdot}68\times 10^{-19}\sqrt{(T_c^{\frac{3}{4}}\mathscr{J}_*)}. \tag{66}$$

Thus if the initial density distribution of the neutral gas is of the form $\rho_0 = \omega_0/r$, and ω_0 and the photon output of the star are related by equation (66) then an ionization front (strong R-type) will travel into the neutral gas with a speed given by expression (63).

One notices that the speed at which the front propagates is proportional to $T_c^{\frac{1}{2}}$ rather than $T_*^{\frac{1}{2}}$ as was previously found in §6. Table 5 gives the values of ω_0 and U_i for each type of star for which the above description of the flow pattern would be applicable. The values of the photon output per unit length of cylinder ($2\pi J_* R_* = 2\pi\mathscr{J}_*$), which have been used, are those calculated from equation (34) and tables 1 and 3.

The density ratio ρ/ρ_i, the gas velocity ratio u/u_i and the ratio $Jr/J_* R_*$ are plotted in figure 5. It will be noticed that the density ratio levels out towards the centre to a value a little greater than $\frac{1}{2}$.

We next calculate the values of ω_0 for which a shock wave will propagate ahead of the ionization front. As in § 6 we will assume that the shock wave is strong. In figure 4 a strong shock is represented by the point B. We follow in the direction of increasing η the integral curve (representing a solution of the differential equations (60) and (61)) through B to some point C, say, which gives the values of $\mathscr{U}_n$ and $\mathscr{A}_n$. These values are now substituted in equation (25), which determines the conditions behind a D-type ionization front: the D i.f. curve as shown in figure 4. It cuts the integral curve AE at D, from this point we follow the

TABLE 5

type of star	$O5$	$O7$	$O9$	$B0$	$B2$
$10^2\omega_0$	4·72	1·09	0·37	0·11	0·05
U_i(km/s)	25·8	24·2	22·8	22·1	21·4

integral curve in the direction η increasing to infinity. The speed of the ionization front is calculated immediately from a knowledge of point D, and the speed of the shock can be calculated by substituting the $(\mathscr{U},\mathscr{A})$ relationship represented by the curve BC in either of the equations (60) and (61) and then integrating. ω/ω_0 is calculated by integrating the differential equations (62) and (55) along the two sections BC and DE (continued to infinity),

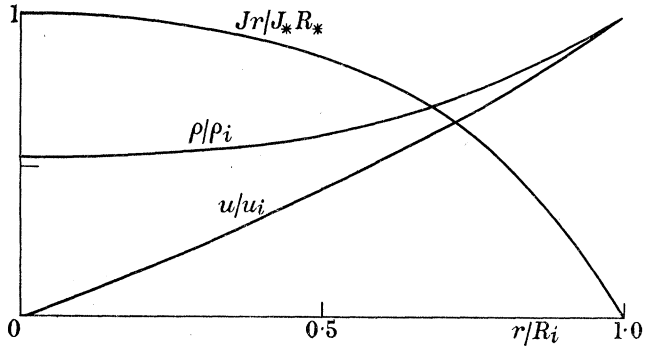

FIGURE 5. Density ratio ρ/ρ_i, velocity ratio u/u_i, and $Jr/J_* R_*$ for the case when an ionization front travels by itself.

respectively. By substituting the variation of ω/ω_0 in equation (65), we can determine the approximate value of w_0 for which this particular model is appropriate. In figure 6 the values of U_i/U_s (corresponding to the selection of the point C) and $\omega_0 10^{19}/\sqrt{(T_c^{\frac{3}{4}}\, \mathscr{J}_*)}$ are plotted for various values of $U_i\sqrt{(M/(2kT_c))}$. In figure 6 one notices that the minimum value of U_i/U_s is 0·81, so that the disturbed neutral gas surrounding the ionized region propagates as a thin shell of material headed by the shock. The gas velocity, pressure and density distributions are shown plotted in figure 7. In table 6 the values of the ionization front velocity, shock velocity and temperature T_s of the gas behind the shock are given for various values of the parameter ω_0 relevant to the particular distributions given in figure 7. Several features of these results are worth noting and can be seen in figure 7. First, the density distribution shows that most of the gas is concentrated in a narrow region just outside the ionization front, whilst the gas in the ionized region is approximately uniform and small.

Secondly, the pressure in the ionized region is approximately equal to the pressure behind the shock; this is consistent with the idea that the thin shell of material surrounding the ionized gas is expanding at a constant rate. Another feature about the solution can be seen from table 6. The temperature behind the shock for case (*a*) is of the order of 5000 to 8000 °K, so that it may be necessary to take into account cooling mechanisms such as dissociation of the neutral gas. For more extreme cases than case (*b*), where the temperature behind the shock varies from 800 to 1100 °K, the shock can no longer be assumed to be a strong shock; the analysis could be modified to include this effect.

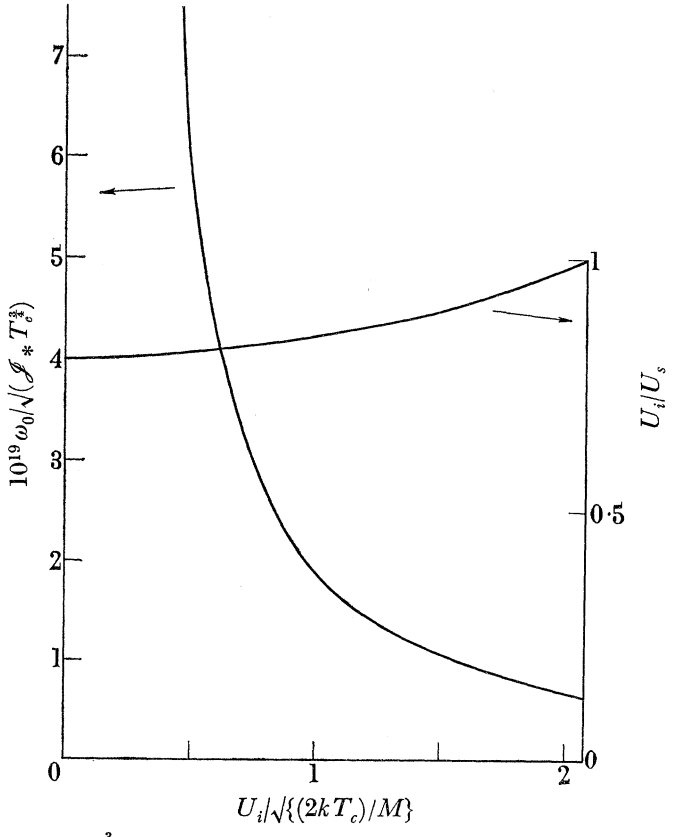

FIGURE 6. $10^{19}\omega_0/\sqrt{(\mathscr{J}_* T_c^{\frac{3}{4}})}$ and U_i/U_s plotted against $U_i/\sqrt{\{(2kT_c)/M\}}$ (cylindrical case).

Our next task is to find out what happens when $\omega_0/\sqrt{(\mathscr{J}_* T_c^{\frac{3}{4}})} < 0{\cdot}68 \times 10^{-19}$. It is clear that for this case we must suppose the existence of some discontinuity within the H II region. However, we have already shown that in the ionized gas the temperature is always equal to T_c; there must therefore be a narrow region behind such a discontinuity if it exists in which the temperature is adjusted to T_c. If we include this narrow region, where adjustment takes place, in with the discontinuity then the resulting discontinuity could be termed an 'isothermal' shock where the temperature on both sides is equal to T_c. Using suffixes i_1, i_2 to label quantities on the star side and ionization front side of the 'isothermal' shock, respectively, then the data are related by the equations

$$\omega_{i_1}(1-\mathscr{U}_{i_1}) = \omega_{i_2}(1-\mathscr{U}_{i_2}), \tag{67}$$

$$\frac{3\mathscr{A}_{i_1}^2}{(1-\mathscr{U}_{i_1})} - 5\mathscr{U}_{i_1} = \frac{3\mathscr{A}_{i_2}^2}{(1-\mathscr{U}_{i_2})} - 5\mathscr{U}_{i_2}, \tag{68}$$

$$\mathscr{A}_{i_1}^2 = \mathscr{A}_{i_2}^2, \tag{69}$$

where ω, $\mathscr{U}$ and $\mathscr{A}$ are the similarity forms in expressions (14) and (15). For the gas to come to rest at the star the point $(\mathscr{U}_{i_1}, \mathscr{A}_{i_1})$ must be on the integral curve marked AE in figure 4. Thus, given such a point we can calculate $\mathscr{U}_{i_2}$ from equation (68). The locus of the points $(\mathscr{U}_{i_2}, \mathscr{A}_{i_2})$ is referred to as the 'isothermal' shock curve and in figure 4 it is represented by the curve FGH and is marked 'i.s.' We now follow the integral curves through points of this i.s.

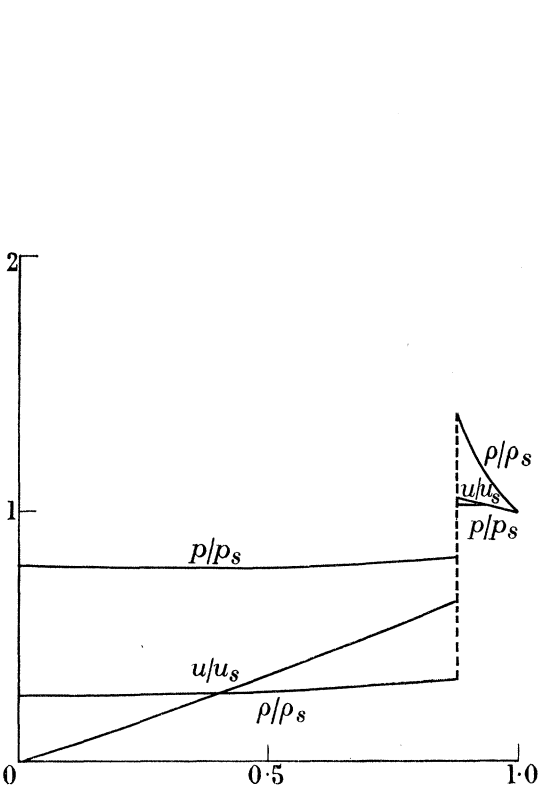

FIGURE 7(a)

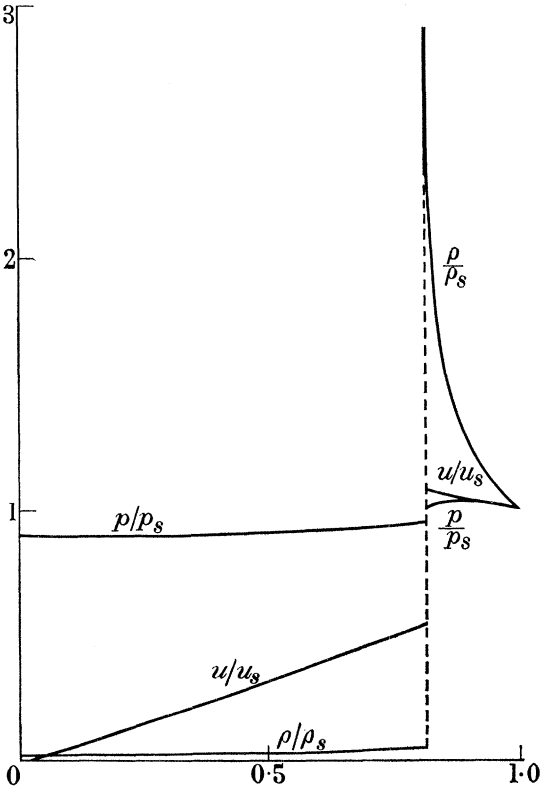

FIGURE 7 (b)

FIGURE 7. Gas velocity, pressure and density distribution (– – – – – denotes the position of the ionization front).

TABLE 6

type of star	O5		O7		O9		B0		B2	
	(a)	(b)	(a)	(b)	(a)	(b)	(a)	(b)	(a)	(b)
$10^2\omega_0$	9·03	51·05	2·09	11·79	0·71	4·00	0·21	1·19	0·10	0·54
U_i(km/s)	16·2	5·8	15·2	5·5	14·4	5·1	13·9	5·0	13·5	4·8
U_s/U_i	1·14	1·23	1·14	1·23	1·14	1·23	1·14	1·23	1·14	1·23
T_s(°K)	7730	1150	6810	1010	6040	910	5650	850	5320	790

curve in the direction η-decreasing. It will be seen from figure 4 that the integrals curves starting at points within the small section FG meet the 'R.i.f.' curve. Thus a flow pattern, which seems to be a possibility in this case, could be described by an ionization front (weak R-type corresponding to a weak detonation) propagating into the neutral gas with an isothermal shock following it in the ionized gas. The values of ω_0, shock and ionization front velocities can be calculated in the way already described. In figure 8 the gas velocity, pressure and density distributions are shown plotted for the particular case when $\omega_0 = 0{\cdot}61 \times 10^{-19}\sqrt{(\mathscr{J}_* T_c^{\frac{3}{4}})}$. The speed of the ionization front U_i is $4{\cdot}7\sqrt{(2kT_c/M)}$ cm/s,

while that of the 'isothermal' shock is $2\sqrt{(2kT_c/M)}$ cm/s. By substituting this speed in the normal Rankine–Hugoniot shock relations we can calculate the strength of the shock which would propagate at the given speed and with conditions ahead represented in figure 4 by the point $(\mathscr{U}_{i_2}, \mathscr{A}_{i_2})$. We find that $p_s/p_{i_2} = 1{\cdot}1$, where p_s is the pressure immediately behind

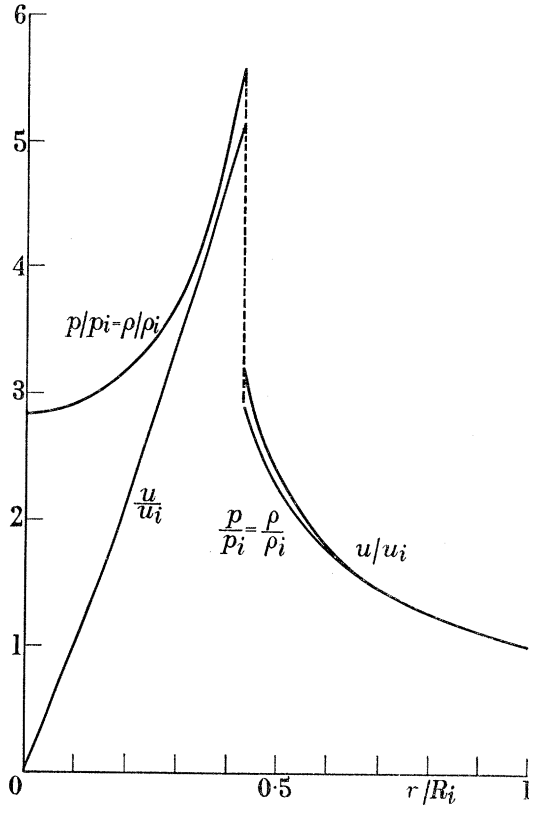

FIGURE 8. Gas velocity ratio, density and pressure ratio plotted as a function of r/R_i. – – – – – – – – denotes the position of the isothermal shock.

the shock (not 'isothermal'). The 'isothermal' shock could therefore be regarded as a weak shock followed by a region in which the temperature is adjusted to T_c. A glance at figure 4 will reveal that the speed of such a discontinuity is always about the same as that calculated for the case when an ionization front travels by itself. Thus the speed will be in the region of 20 to 30 km/s, depending upon the type of radiating star. The rate of expansion of the whole ionized region is not limited and varies from that given by expression (63) to infinity. The values of ω_0 vary according to the flow pattern which is assumed.

As in § 6 there are other flow patterns which could be considered, such as those in which a shock leads the ionization front which is followed by an isothermal shock. Referring to figure 4, we see that for a fixed relative velocity between the shock and the ionization front (i.e. corresponding to fixing the point C) we could follow the integral curve from D in the direction η increasing *or* we could follow any one of the integral curves (say OIJ) which intersect the D i.f. curve in the region bounded by HGF, FO and the negative U-axis. In the latter case the flow pattern would include an 'isothermal' shock in the ionized gas. Thus the question of uniqueness shows itself again and this can only be settled by considering the structure of ionization fronts in great detail. This is discussed by Axford in the next paper where it is shown how one can obtain the unique solution in any given case.

Finally, it is worth noticing that the temperature variation in the ionized gas could be determined, since knowing $\mathscr{U}$ and η we can find F (see expression (57)). Equations (38) (neglecting the $\mathrm{d}x/\mathrm{d}\eta$ term) and (42) then determine the temperature distribution. It is found that the variation in the ionized region is about 5 °K and is therefore negligible. The degree of ionization can also be found and here again the error in assuming that x is approximately equal to 1 is small.

8. Spherical ionization fronts (II)

Finally, we consider the expansion of a spherical ionized region using as a working basis the approximate ideas developed in § 7. The results of §§ 6 and 7 have shown that recombination and cooling cannot be neglected even at the ionization front. The analysis of § 6 must therefore be re-examined and an effort made to include these effects. We note first that restriction (ii) is no longer applicable since it followed from equation (9) which assumed that no recombination or cooling at the front took place. This means that the similarity form for the density could be other than that given by expression (14). In fact, in order to take into account recombination, the similarity form is determined by the approximate equation

$$J_* R_*^2 = \frac{\beta}{M^2}\int_0^{R_i} \rho^2 r^2 \,\mathrm{d}r, \tag{70}$$

which like equation (65) assumes that much of the radiation has been absorbed in the ionized gas before it reaches the ionization front. Since $J_* R_*^2$ is a constant, equation (70) implies that, for a similarity solution to be applicable, $\rho r^{\frac{3}{2}}$ must be a function of the similarity variable t/r, namely $\omega(\eta)$. Thus we now solve the spherical problem, taking into account cooling and the re-ionization of recombined atoms in the H II region, for the case when the initial density distribution varies according to the law $\rho_0 = \omega_0/r^{\frac{3}{2}}$. The analysis is similar to that described in § 7 so that only brief details will be given. The differential equations describing the motion in the ionized gas for this case are

$$D_1 \eta \frac{\mathrm{d}\mathscr{U}}{\mathrm{d}\eta} = \mathscr{U}(1-\mathscr{U})^2 - \tfrac{3}{2}(2\mathscr{U}-1)\,\eta^2, \tag{71}$$

$$\frac{D_1 \eta}{\omega}\frac{\mathrm{d}\omega}{\mathrm{d}\eta} = \tfrac{3}{2}\eta^2 - \tfrac{1}{2}\mathscr{U}(1-\mathscr{U}), \tag{72}$$

where $D_1 = (1-\mathscr{U})^2 - \eta^2$. $\mathscr{A}$ is given by expression (56), and equation (71) is solved in the $(\mathscr{U},\mathscr{A})$-plane. The differential equations applicable in the H I region are

$$D\eta \frac{\mathrm{d}\mathscr{U}}{\mathrm{d}\eta} = \mathscr{U}(1-\mathscr{U})^2 + 3\mathscr{A}^2\left(\tfrac{3}{5} - \mathscr{U}\right), \tag{73}$$

$$\frac{D\eta}{\mathscr{A}}\frac{\mathrm{d}\mathscr{A}}{\mathrm{d}\eta} = (1-\mathscr{U})^2 - \tfrac{2}{3}\mathscr{U}(1-\mathscr{U}) - \left[1 - \tfrac{3}{10}(1-\mathscr{U})^{-1}\right]\mathscr{A}^2, \tag{74}$$

$$\frac{D\eta}{\omega}\frac{\mathrm{d}\omega}{\mathrm{d}\eta} = \frac{3(\frac{3}{5}-\mathscr{U})\mathscr{A}^2 - \mathscr{U}(1-\mathscr{U})^2}{2(1-\mathscr{U})}, \tag{75}$$

where $D = (1-\mathscr{U})^2 - \mathscr{A}^2$. Figure 9 shows some of the integral curves which represent solutions of equation (71) in the $(\mathscr{U},\mathscr{A})$-plane (note that $\mathscr{A} = \sqrt{(5/3)}\,\eta$). The integral curve labelled BCM is a solution of equations (73) and (74) with η eliminated and the curve goes

through the strong shock point B. By varying the point C on the curve BM, one can obtain solutions corresponding to different positions of the ionization front relative to the shock wave.

When the H II region is headed by a strong R-type ionization front with no shock in front, the solution is given by the integral curve ADE in figure 9. From a knowledge of the point A and by integration of equation (70), the speed of the ionization front and the appropriate value of ω_0 are found to be

$$U_i = \sqrt{\frac{2kT_c}{0{\cdot}24M}}, \quad \omega_0 = 0{\cdot}844 \times 10^{-19} \sqrt{(T_c^{\frac{3}{4}} J_* R_*^2)}. \tag{76}$$

Comparing the first of these expressions with equation (63) one notices that the speed of the ionization front is almost the same as for the cylindrical case. Again we find that the

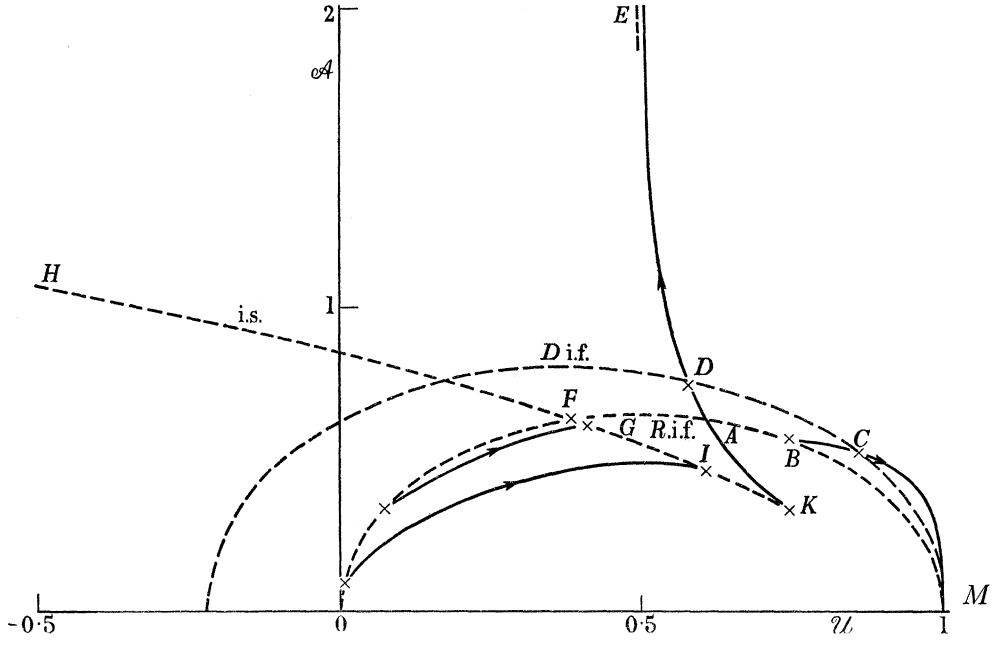

FIGURE 9. The $(\mathscr{U},\mathscr{A})$-plane representing the solution of differential equations (71), (73) and (74) (spherical motion).

strong R-type ionization front propagates with a speed such that the gas velocity immediately behind it is approximately equal to the local speed of sound, i.e. $u_i = \sqrt{(10kT_c/3M)}$. One must not, however, interpret this as meaning that all strong R-type ionization fronts will propagate at such a speed that the above result is true, as it depends on the choice of $\frac{5}{3}$ for γ; the approximate equations of motion are independent of this choice. A comparison between the densities is difficult because of the different assumptions made regarding the density of the neutral gas initially, namely like $1/r$ in the cylindrical case and like $1/r^{\frac{3}{2}}$ in the spherical case. A plot of the density and fluid velocity distributions in the H II region yields results similar to those shown in figure 5.

Calculations could now be made which would determine the values of the parameter ω_0 for which a shock wave will propagate ahead of the ionization front. Such calculations would yield substantially the same results as for the cylindrical case. Figure 10 shows the values of $10^{19}\omega_0/\sqrt{(J_* R_*^2 T_c^{\frac{3}{2}})}$ and U_i/U_s plotted against $U_i/\sqrt{\{(2kT_c)/M\}}$.

For a given value of ω_0 and given type of star, the shock and ionization front velocity can be read off. The ionization fronts in all these cases are D-type if we regard the strong R-type ionization front as being a D-type initiated by a shock wave. Again there is a value of $\omega_0/\sqrt{(J_* R_*^2 T_c^{\frac{3}{4}})}$ below which the above description of the flow is no longer applicable. For these cases the presence of 'isothermal' shocks within the H II regions must be assumed. The general observations made regarding these in § 7 still apply in the spherical case. The question of uniqueness and the possibility of the existence of weak R-type ionization fronts

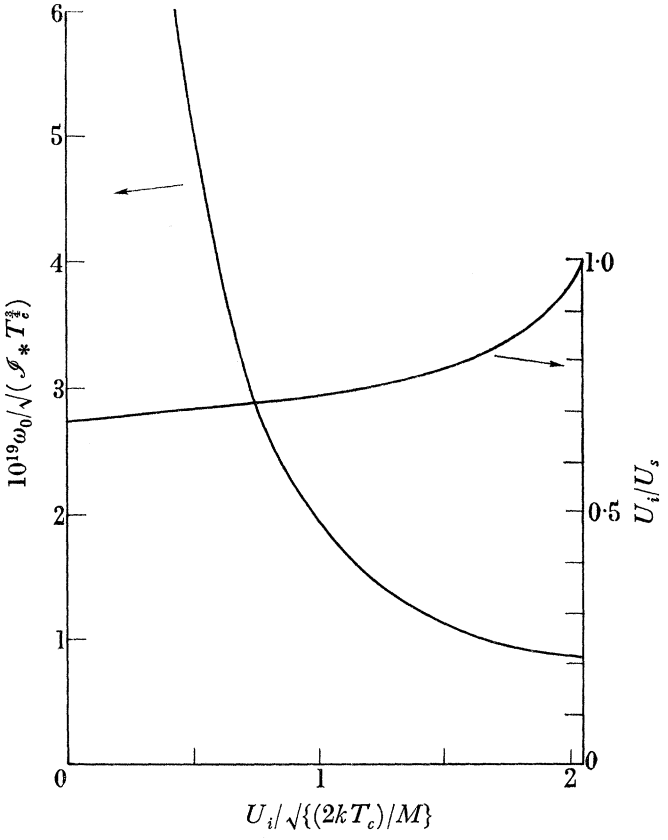

FIGURE 10.

are raised again. One slight difference will be observed when figure 9 is compared with figure 4. The integral curves, starting at points on the section OF of the R i.f. curve and for which $U < 0{\cdot}25$, lie to the right of the R i.f. curve. This means that lower speeds of the 'isothermal' shock may be possible in spherical geometry than were possible in cylindrical geometry (transitions across an 'isothermal shock' from points on FK to points on AK have to be considered in the spherical case).

CONCLUSIONS

It is true that the solution which has been described in this paper is an idealization of the problem of determining the effect of a star's radiation on the surrounding interstellar gas. A particular initial density distribution has been assumed in order that similarity of the flow pattern at differing times may be used to put the differential equations in a form which allows fairly easy integration. However, several conclusions can be drawn from the analysis and an overall picture of the flow in a real problem can be obtained. The analysis has

revealed what type of discontinuities may be expected to occur; for instance, it has told us that at speeds less than about $\sqrt{(2kT_c/0{\cdot}23M)}$, a shock may be expected to move ahead of the ionization front, while for speeds greater than this an 'isothermal' shock may occur within the H II region. Though the value quoted here is strictly true for the case of similarity only, the order of magnitude of the velocity, at which the character of the flow is changed, is probably correct, since $\sqrt{(2kT_c/M)}$ is the fundamental speed involved in the problem. Thus, for any initial density distribution of the neutral gas and when the similarity hypothesis is no longer true, the following description of the flow from the time the star begins to emit ionizing radiation is suggested. Initially a weak *R*-type ionization front moves out with a fast speed, followed by an 'isothermal' shock which moves with a speed of about $\sqrt{(2kT_c/M)}$. The ionization front slows down. Two possible flow patterns become possible. Either a shock wave moves away from the ionization front leaving a strong *D*-type ionization front behind or the isothermal shock catches up the ionization front and the interaction leads to a strong *R*-type ionization front moving with a speed of order $\sqrt{(2kT_c/M)}$. If the former is the case then at a later stage the isothermal shock will catch up with the strong *D*-type ionization front and a weak *D*-type ionization front is formed. If the latter is the case then a shock wave emerges from the strong *R*-type ionization front leaving a weak *D*-type ionization front behind. Both yield the same final flow pattern, which ultimately becomes that studied by Strömgren (1939) and the H II region has dimensions of the Strömgren sphere.

The author wishes to thank Dr F. D. Kahn for the many valuable discussions on the subject he has had with him and at whose suggestion this work was undertaken. He is also indebted to his co-worker I. Axford for his development of the subject.

References

Allen, C. W. 1955 *Astrophysical Quantities*, p. 89. University of London: Athlone Press.
Axford, W. J. 1961 *Phil. Trans.* A, **253**, 301.
Kahn, F. D. 1954 *Bull. astr. Insts Netherlds*, **12**, 187 (no. 456).
Kahn, F. D. & Schatzman, E. 1955 *Gas dynamics of cosmic clouds* (*I.A.U. Symp.* no. 2), p. 163, Amsterdam: North-Holland Publ. Cy.
Pottasch, S. 1958 *Bull. astr. Insts Netherlds*, **14**, 29 (no. 482).
Spitzer, L. 1954 *Astrophys. J.* **120**, 1.
Strömgren, B. 1939 *Astrophys. J.* **89**, 526.
Struve, O. 1950 *Stellar evolution*, chap. ii. Princeton University Press.
Taylor, G. I. 1946 *Proc. Roy. Soc.* A, **186**, 273.

PHILOSOPHICAL TRANSACTIONS OF THE ROYAL SOCIETY A MATHEMATICAL, PHYSICAL & ENGINEERING SCIENCES